Fabrication of Yttria-Doped Zirconia-Alumina Composite Ceramics with High Strength and Fracture Toughness by Pulsed Electric-Current Pressure Sintering

Ken HIROTA*, Kenta YAMAMOTO, Koki SASAI, Masaki KATO*, Hideki TAGUCHI**,

Hideo KIMURA, Masayuki TAKAI, and Masao TERADA***

ZrO_2-Al_2O_3 composite ceramics containing 10~30 mol% Al_2O_3 and 1.5 mol% Y_2O_3, *i.e.*, 90~70 mol% ZrO_2 (1.5 mol% Y_2O_3)-10~30 mol% Al_2O_3 ceramics, have been fabricated by pulsed electric-current pressure sintering (PECPS) of cubic ZrO_2 solid solution(*ss*) nano-powders prepared via the neutralization co-precipitation method, at 1598 K for 600 s under 50~60 MPa in Ar. Y_2O_3-doped tetragonal-ZrO_2 (*ss*)/α-Al_2O_3 dense ceramics were composed of 280-130 nm grains. FE-SEM observation revealed that their microstructures, that is the grain sizes of both *t*-ZrO_2(*ss*) and α-Al_2O_3, and the distribution of α-Al_2O_3 grains, were much influenced by the content of α-Al_2O_3. The best mechanical properties of extreme high bending strength ($\sigma_b \geq 1$ GPa) and high fracture toughness ($K_{IC} \geq 15$ MPa·m$^{1/2}$) were attained simultaneously at the composition of 25 mol% Al_2O_3 with a high relative density of 99.9%, as the same composition reported on the hot isostatic press (HIP) sintered ZrO_2 (2~3 mol%Y_2O_3)-Al_2O_3 composite ceramics.

Key words: Zirconium oxide (ZrO_2), aluminum oxide (Al_2O_3), solid solution, neutralization co-precipitation method, pulsed electric-current pressure sintering (PECPS)

1. Introduction

Table 1 shows the representative mechanical properties of various kinds of partially stabilized ZrO_2 (PSZ) ceramics reported before; it is easy to notice that high bending strength (σ_b) is attained in Y_2O_3-doped ZrO_2 (Y-PSZ)[1-3] and high fracture toughness K_{IC} in Al_2O_3-doped ZrO_2 (Al-PSZ)[4], and that both properties could not be realized in the same PSZ.

Table 1. Mechanical properties of ZrO_2 (*ss*) ceramics reported previously.

	Content of additives (mass%)	Vickers hardness H_V (GPa)	Young's modulus E (GPa)	Bending strength σ_b (MPa)	Fracture toughness K_{IC} (MPa · m$^{1/2}$)
Y-PSZ *(Y_2O_3)	5	13.6	233	1384	6.9
Ca-PSZ* (CaO)	9	17.2	210	241	2.5
Mg-PSZ* (MgO)	2.8	14.4	200	685	4.8
Al-PSZ** (Al_2O_3)	25 [mol%]	—	—	570	23

*Partially Stabilized Zirconia
**Ceramics sintered by HIP (200 MPa/1100°C/1h) using ZrO_2-25mol%Al_2O_3 (*ss*) powders prepared from sol-gel method. : Powder Metallurgy World Congress (1993) 1381-1384.

* Department of Molecular Science & Technology, Faculty of Engineering, Doshisha University, Kyotanabe, Kyoto 610-0321, Japan, Tel: +81-774-65-6690, Fax : +81-774-65-6849, E-mail:khirota@mail.doshisha.ac.jp
** Graduate School of Natural Science and Technology, Okayama University, Okayama 700-8530, Japan, Tel/Fax: +81-86-251-7901, +81-86-284-6163, E-mail: htaguchi@okayama-u.ac.jp
***Daiichi Kigenso Kagaku Kogyo Co., Ltd., Suminoe-ku Hirabayashi-minami, Osaka 559-0025, Japan, Tel:+81-6-6682-1265 FAX: +81-6-6682-8939, E-mail: kimura-h@zr.dkkk.co.jp

However, in 2012, it was reported that dense $ZrO_2(Y_2O_3)$-25 mol%Al_2O_3 composite ceramics fabricated by pulsed electric-current pressure sintering (PECPS)[5-7] of sol-gel derived cubic ZrO_2 solid solution(ss) powders showed extreme high strength ($\sigma_b \geq 1$ GPa) and high toughness ($K_{IC} \geq 20$ MPa·m$^{1/2}$) simultaneously, which broke the above mentioned common sense for the first time[8-10]. And then in 2013, the solid solution powders with the compositions of ZrO_2 (0.5~2.0 mol% Y_2O_3)-25 mol% Al_2O_3 prepared by the neutralization co-precipitation method[11] were compacted and densified by the PECPS; this powder preparation method can produce relatively homogeneous powders with high productivity at low cost in comparison with the sol-gel method. It has been clarified that the composite ceramics thus fabricated showed high mechanical properties of ($\sigma_b \geq 1$ GPa) and high fracture toughness ($K_{IC} \geq 15$ MPa·m$^{1/2}$) at the 1.5 mol% Y_2O_3 composition[12]; this composition was based on the previously reported ZrO_2 (2.0~3.0 mol% Y_2O_3)-Al_2O_3 composite ceramics with high mechanical properties, those were fabricated using conventional norma sintering, hot pressing (HP) or hot isostatic pressing (HIP)[13-16].

However, in comparison with the previous works[13-16], the powder preparation method has been changed, i.e., from a solid state reaction to liquid phase methods (sol-gel or neutralization co-precipitation), the maximum content of Y_2O_3 from 2~3 to 1.5 mol%, and sintering methods are also changed from HP or HIP with the heating rate of about 300 K·h^{-1} to PECPS with 100 K·min^{-1}. In the present study, based on these circumstances and from the viewpoint of finding the suitable content for Al_2O_3 to attain high mechanical properties, the effect of Al_2O_3 content on the microstructure of the composite ceramics was investigated.

2. Experimental

2.1 Preparation of ZrO_2 (1.5 mol%Y_2O_3)-y·mol%Al_2O_3 (y=10, 20, 25, 30) ceramics

Fig. 1 shows the flowchart for the fabrication of $ZrO_2(Y_2O_3)$-Al_2O_3 composite ceramics.
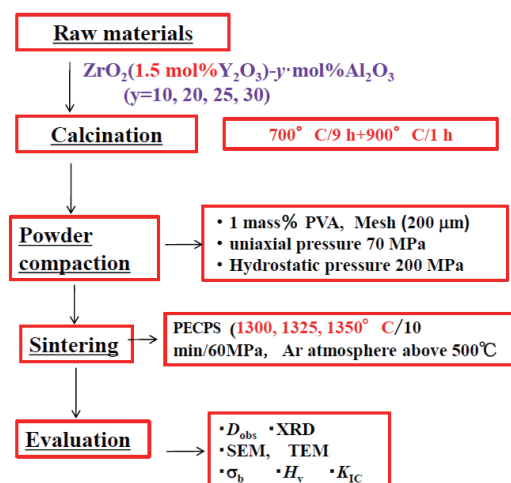
Fig. 1. Flowchart for the fabrication of ZrO_2(1.5Y) y·mol%Al_2O_3 ceramics.

The preparation of powders and the fabrication of dense ceramics using these powders are described in previous our paper[12]. The solid solution(ss) powders with the composition of (100-y)·mol%ZrO_2(1.5mol% Y_2O_3)-y·mol%Al_2O_3 (y=10, 20, 25, 30) were prepared by the neutralization co-precipitation method[11] (after this, these powders are denoted as 10A, 20A, 25A, and 30A). Based on the data shown in Fig. 2 (as described in the later), the as-prepared amorphous powders (precursor) were heated in air at 973 K for 32.4×10^3 s, and subsequently followed by the heat treatment at 1173 K for 3.6×10^3 s; these calcination conditions were determined by the crystallization temperatures about 1083 K from the results of XRD and DTA/TG analyses, as described in the later. The lower-temperature heating treatment was adopted to enhance the homogeneity of elemental-distribution in the particles prepared by the neutralization co-precipitation method. The higher-temperature heating treatment was to crystalize the precusors to improve their sinterablity.
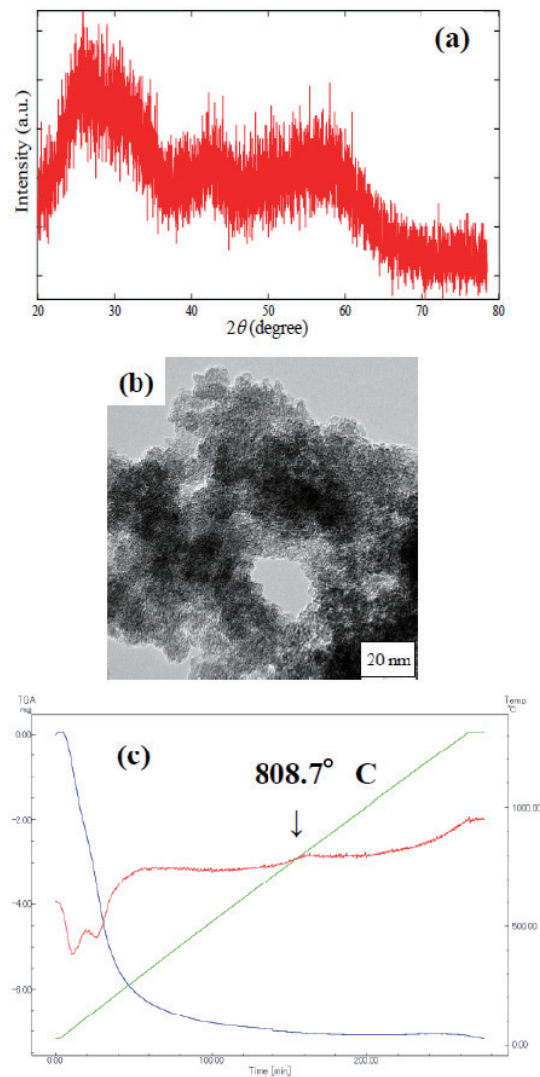
Fig. 2. Some characteristics of as-prepared powder corresponding to the composition of 80 mol% ZrO_2(1.5Y)-20mol%Al_2O_3: (a) XRD pattern, (b) TEM photograph and (c) DTA/TG curves.

Calcined powder compacts (density: 2.2~2.4 $Mg \cdot m^{-3}$) after cold isostatic pressing (CIPing) at 245 MPa for 3 min were sintered with a pulsed electric-current pressure sintering (PECPS: *SPS-5104A*, SPS SYNTEX INC., Tokyo, Japan) (on-off interval=12:2) with a heating rate of 100 $K \cdot min^{-1}$, at 1598 K under 50~60 MPa in Ar for 600 s using a carbon mold (ϕ40-ϕ16-30^h mm) and plunger (ϕ39.9-40^h mm).

2.2 *Characterization and evaluation*

Thermal analysis of precursors was conducted using a differential thermal analysis and thermal gravimetry (DT-TG 60H, Shimadzu, Kyoto, Japan) in air with a heating rate of 0.1667 $K \cdot s^{-1}$ (10 $K \cdot min^{-1}$). Crystalline phases were identified by X-ray diffraction (XRD) analysis (Cu$K\alpha_1$ radiation, *Rint 2000*, Rigaku, Osaka, Japan). The volume fraction of the monoclinic ZrO_2 (*m*-ZrO_2) phase for the test samples was determined from the intensity ratio of the monoclinic (111) and (11-1) diffraction lines to the tetragonal (111) line by XRD analysis[17]. Bulk densities (D_{obs}) of sintered ceramics after polishing with a diamond paste (nominal size ϕ1~3 μm) were evaluated by Archimedes method.

Microstructural observation on the as-prepared and calcined powders, and the fractured or polished surfaces of ceramics were conducted using a field emission-type transmission electron microscope (FE-TEM, *JEM-2100F*, JEOL Ltd., Tokyo, Japan) and a scanning electron microscope (FE-SEM, *JSM-7001FD*, JEOL Ltd.) equipped with an energy dispersive spectroscopy (EDS, *JED-2300/T* and *JED-2300/F*, JEOL Ltd., respectively). Before TEM observation, the specimens were processed into thinner using a focused ion beam (FIB, *FB-2200*, Hitachi High-Tech Fielding Co. Ltd., Tokyo, Japan). The grain sizes were determined using an intercept method[18].

After crystalline phase identification, test bars (~3×3.5×11 mm^3) for mechanical-property measurements were cut from the ceramics with a diamond cutting-blade and then their four sides were polished to mirror surface with a diamond paste (nominal particle size ϕ1-3 μm). Three-point bending strength (σ_b) was evaluated with a cross-head speed of 0.5 mm$\cdot$min^{-1} and using an 8 mm-span length WC jigs. Vickers hardness (H_v) and fracture toughness (K_{IC}) were evaluated using a Vickers hardness tester (*HMV*, Shimadzu) with an applying load of 19.6 N and a duration time of 15 s for the former, and the indentation fracture method (IF) with Niihara's equation[20] using a Vickers hardness tester (*VMT-7*,

Matsuzawa, Osaka, Japan) with applying load of 196 N and a duration time of 15 s for the latter.

3. Results and Discussion

3.1 *Characteristics of powders*

After drying at 393 K, the as-prepared powders were characterized; Fig. 2 (a) shows the XRD pattern and (b) TEM image of 20A powder as a representative example. All as-prepared powders were amorphous and their particle sizes P_s were very fine, *i.e.*, about 3~5 nm. Their BET specific surface areas of 140~180 $m^2 \cdot g^{-1}$ support the above mentioned values. Fig. 2 (c) shows the DTA/TG curves of 20A; an exothermic peak around 1082 K was observed. This temperature is recognized to correspond to the crystallization temperature T_x from our previous study[12]. From the DTA/TG data, it was clear that with increasing Al_2O_3 content, T_x increases monotonously; 953 K (10A), 1082 K (20A), 1083 K (25A), and 1085 K (30A powder). By comparing with the data obtained for Sol-gel derived powders: T_x (sol-gel 25A) ~1093 K[10] and T_x (sol-gel 25A without Y_2O_3) ~1043 K[21], it becomes clear that i) 1.5mol% Y_2O_3 addition rises T_x about 50 K, and ii) the neutralization co-precipitated powder reveal a lower T_x than that of Sol-gel powder.

By the XRD analysis, the crystalline phases of powders calcined at 973 K for 32.4×10^3 s and 1173 K for 3.6×10^3 s were identified to be only cubic ZrO_2 phase (JCPDS: #49-1642) with broad diffraction peaks as shown in Fig. 3. These results indicate that cubic ZrO_2 solid solutions (c-ZrO_2 (ss)) those contain both Al_2O_3 and Y_2O_3 were formed from the amorphous powders prepared *via* the neutralization co-precipitation method; conventional solid state reaction process cannot produce these c-$ZrO_2(ss)$. TEM photographs of the calcined powders are displayed in Fig. 4, showing that with increasing the Al_2O_3 content,

their P_s decreased around 15 to 6.5 nm as the same behavior as the as-prepared powders.

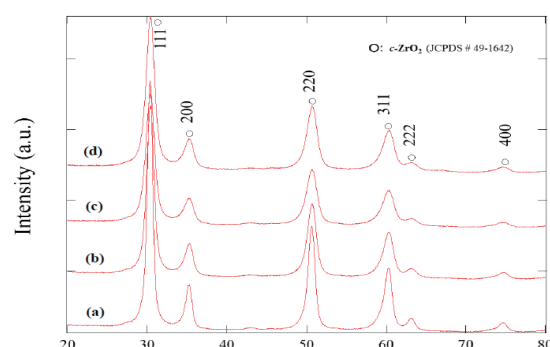Fig. 3. XRD patterns of calcined powders corresponding to the compositions of $(ZrO_2(1.5Y)$-$y \cdot mol\%$ $Al_2O_3)$: y=10, 20, 25 and 30.
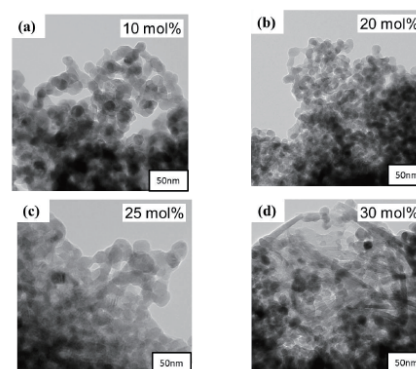
Fig. 4. TEM photographs of $ZrO_2(1.5Y)$-$y \cdot mol\% Al_2O_3$.

From XRD analysis, the lattice parameter a of calcined c-$ZrO_2(ss)$ powders was determined to be almost constant of 0.509~0.508 nm, nevertheless, a: 0.510 → 0.512 nm for the Sol-gel powders with increasing Al_2O_3 content.

3.2 *Microstructures and mechanical properties of ceramics*

Calcined powder compacts were densified using a PECPS as already described. Fig. 5 shows representative XRD patterns of the polished surfaces of ceramics sintered at 1598 K under 50~60 MPa in Ar for 10 min; a main phase changed from c-$ZrO_2(ss)$ to tetragonal t-ZrO_2, monoclinic m-ZrO_2 and α-Al_2O_3.

Diffraction peaks are indexed based on each PDF file (t-ZrO_2: #50-1089, m-ZrO_2: #37-1481, α-Al_2O_3: #10-0173).
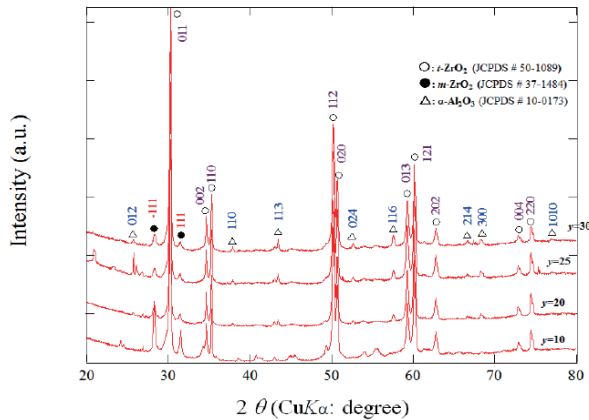
Fig. 5. XRD patterns for ZrO_2(1.5Y)-$y\cdot$mol%Al_2O_3 ceramics: y=10, 20, 25 and 30.

From these XRD line intensity data, t-ZrO_2 $vs.$ m-ZrO_2 phase vol% was calculated using Garvie & Nicholson's equation[17]. And using Rietveld analysis[19], the lattice parameters a: 0.3601, c: 0.5183 nm for t-ZrO_2, and a: 0.5153~0.5165, b: 0.5170~0.5198, c: 0.5324~0.5365 nm β: 98.6~98.9° for m-ZrO_2 phases were evaluated.

Fig. 6 displays SEM (secondary electron image: SEI) photographs for the fractured surfaces of the ceramics.
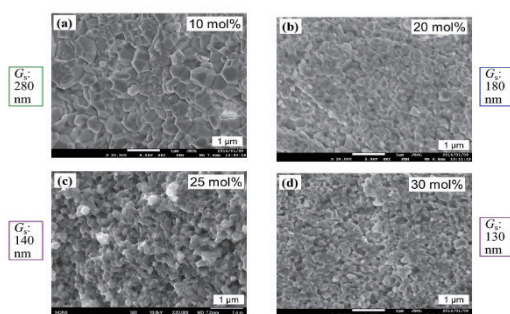

Fig. 6. SEM (SEI) photographs of the fracture surfaces of ZrO_2(1.5Y)-$y\cdot$mol%Al_2O_3 ceramics: y= (a) 10, (b) 20, (c) 25 and (d) 30.

Dense homogeneous microstructure is observed, in addition, grain size G_s of main ZrO_2 phase estimated using an intercept method[18] is also indicated in brackets. The values of G_s decreased from 280 to 130

nm with increasing Al_2O_3 content. As these photographs show only grain morphology, α-Al_2O_3 grains are not distinguished from ZrO_2 grains. By adopting SEM observation using back scattered electron image (BEI), α-Al_2O_3 grains were recognized. Fig. 7 presents these photographs; black dots represent α-Al_2O_3 grains among ZrO_2 matrix. From these, it becomes apparent that i) G_s of α-Al_2O_3 become smaller and ii) homogeneity in α-Al_2O_3 grain distribution better, with increasing the Al_2O_3 content.

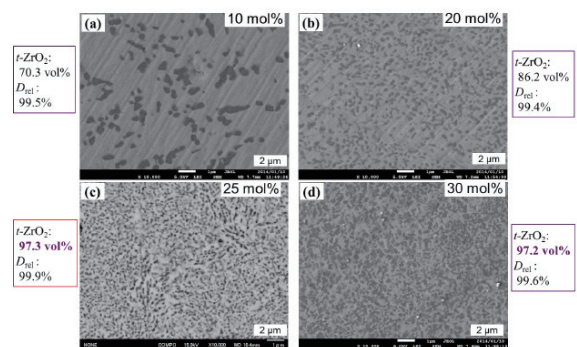Fig. 7. SEM (BEI) photographs of the polished surfaces of ZrO_2(1.5Y)-$y\cdot$mol%Al_2O_3 ceramics: y= (a) 10, (b) 20, (c) 25 and (d) 30.

The ratio of t-ZrO_2 $vs.$ m-ZrO_2 phase in vol% and the relative density (D_{rel}) estimated from the bulk density (D_{obs}) and theoretical density (D_x) are also presented in the brackets. Here, the value of D_x of each ceramics is calculated based on D_x(t-ZrO_2)= 6.07~6.08, D_x(m-ZrO_2)=5.78~5.79, t/m-ZrO_2 phase volume ratios, and D_x(α-Al_2O_3)=3.987 Mg·m^{-3}, $i.e.$, 5.749 (10A), 5.572 (20A), 5.455 (25A), and 5.344 Mg·m^{-3} (30A). It should be noted that with increasing the Al_2O_3 content t-ZrO_2 vol% increased from 70 to 97% around 25A ceramics. High t-ZrO_2 vol% is required to achieve high mechanical properties in addition to high relative density more than 99.5%.

The mechanical properties of three-point bending strength (σ_b), Vickers hardness (H_v) and fracture toughness (K_{IC}) of thus fabricated composite ceramics are measured. Fig. 8 displays (a) σ_b, (b) H_v, and (c) K_{IC} as a function of Al_2O_3 content. It is apparent that 25A

composition gives the best data, such as σ_b: 1355 MPa, (b) H_v: 15.3 GPa, and (c) K_{IC}: 15.9 MPa·m$^{1/2}$. These data are astonishing values from the following viewpoint; i) each value is itself very high: $\sigma_b \geq 1.3$ GPa, $H_v \geq 15$ GPa, and $K_{IC} \geq 15$ MPa·m$^{1/2}$, ii) high values of $\sigma_b \geq 1.3$ GPa and $K_{IC} \geq 15$ MPa·m$^{1/2}$ are achieved at the same composition ceramics.
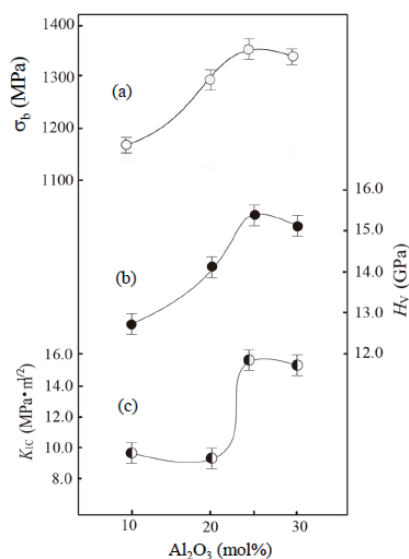

Fig. 8 Mechanical properties of ZrO$_2$(1.5Y)-y·mol%Al$_2$O$_3$ ceramics: (a) bending strength σ_b (MPa), (b) Vickers hardness H_v (GPa), and (c) fracture toughness K_{IC} (MPa·m$^{1/2}$).

The former item is often reported in the PSZ-Al$_2$O$_3$ composite ceramics those were fabricated by hot isostatic pressing (HIP)[16], however, the latter has not been realized up to now except for our studies because the values of σ_b and K_{IC} has a "trade-off" relations in the ceramic field; this has been believed for long time in terms of much difference in atom-bonding, metallic bonding for metals, and ionic or covalent bondings for ceramics with little plastic deformation. However, the present study has proved that both high mechanical properties, both strength and toughness, can be accomplished by fabricating the dense ($\geq$99.9%) fine grained ($\leq$200 nm) composite ceramics, in addition, under the materials design of utilizing t- to m-ZrO$_2$ transformation toughening mechanism.

Fig. 9 explains the additional mechanical property- improving mechanism; a role of α-Al$_2$O$_3$ grains in the ZrO$_2$ matrix.
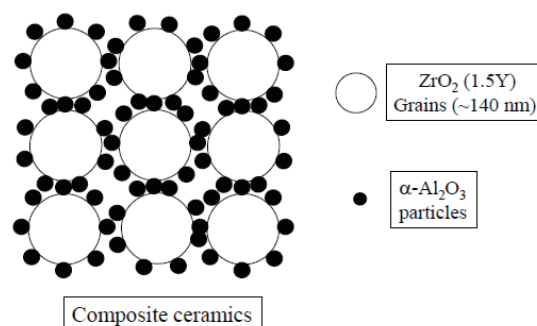

Fig. 9 Schematic view of the additional mechanical property-improving mechanism.

Fine α-Al$_2$O$_3$ grains are homogeneously distributed and surround t-ZrO$_2$ grains; this might be due to the homogeneous precipitation of α-Al$_2$O$_3$ from c-ZrO$_2$(ss) containing 25 mol% Al$_2$O$_3$ and 1.5 mol% Y$_2$O$_3$ during PECPS. These α-Al$_2$O$_3$ grains have much effect on the restraint of t-ZrO$_2$ to m-ZrO$_2$ transformation, even though, a smaller amount of Y$_2$O$_3$ stabilizer than the conventional 2~3 mol%.

4. Summary

Dense and fine-grained ZrO$_2$ (1.5mol%Y$_2$O$_3$)-25 mol% Al$_2$O$_3$ composite ceramics fabricated by PECPS of c-ZrO$_2$(ss) powders prepared via the neutralization co-precipitation method revealed extraordinary high mechanical properties, such as strength $\geq$ 1.3 GPa and toughness $\geq$15 MPa·m$^{1/2}$. These developed properties were brought by their microstructures; high relative density of 99.9%, ~150 nm t-ZrO$_2$(ss) grains surrounded by fine α-Al$_2$O$_3$ grains, and high t-ZrO$_2$ volume ratios $\geq$95%; those items are based on "a material design to fine engineering ceramics".

Kyoto, Japan.

References

1) N. Claussen, "Stress Induced Transformation of Tetragonal ZrO_2 Particles in Ceramic Matrices", J. Am. Ceram. Soc., **61**, 85-86 (1978).

2) R. Ruhle, N. Clausen, and A. H. Heuer, "Microstructural studies of Y_2O_3-containning tetragonal ZrO_2 polycrystal (Y-TZP)", *Advances in Ceramics*, **12**, (American Ceramic Society, Ohio, 1984), pp. 352-370.

3) T. Masaki, "Mechanical properties of toughened ZrO_2-Y_2O_3 ceramics", J. Am. Ceram. Soc., **69**, 638-640 (1986).

4) S. Inamura, M. Miyamoto, Y. Imaida, M. Takagwa, K. Hirota, and O. Yamaguchi, "High fracture toughness of ZrO_2 solid-solution ceramics with nanometre grain size in the system $ZrO_2-Al_2O_3$", J**.** Mater**.** Sci**.** Lett., **12,** 1368-1370 (1993).

5) M. Tokita, "Trend in Advanced SPS Spark Plasma System and Technology", J. Soc. Powder Tech. Jpn., **30,** 790-804 (1993).

6) S. Grasso, Y. Sakka, and G. Maizza, "Electric current activated/assisted sintering (ECAS): a review of patents 1906-2008", Sci. Tech. Adv. Mater., **10** [053001] (2009).

7) R. Orru, R. Licheri, L. Antonio Mario, C. Alberto, and C. Giacomo, "Consolidation/synthesis of materials by electric current activated/assisted sintering", Mater. Sci. Eng. R., **63,** 127-287 (2009).

8) K. Shibaya, H. Sato, H. Matsuda, K. Takaoka, M. Kato, K. Hirota, and H. Taguchi, "Fabrication of ZrO_2 Solid Solution Ceramics Containing Al_2O_3 Having High Bending Strength ($\sigma_b \geq 1$ GPa) and High Fracture Toughness ($K_{IC} \geq 20$ MPa·m$^{1/2}$) Simultaneously by Pulsed Electric-current Pressure Sintering (PECPS)", J. Jpn. Soc. Powder Powder Metall., **58**, 727-732 (2012).

9) K. Hirota, K. Shibaya, H. Matsuda, M. Kato, and H. Taguchi, "Fabrication of novel $ZrO_2(Y_2O_3)$-Al_2O_3 ceramics having high strength and toughness utilizing pulsed-electric current pressure sintering (PECPS)", Advances in Applied Ceramics: Structural, Functional and Bioceramics, **113,** 73-79 (2013).

10) K. Hirota, K. Shibaya, H. Matsuda, M. Kato, and H. Taguchi, "Fabrication of novel $ZrO_2(Y_2O_3)$-Al_2O_3 ceramics having high strength and toughness by pulsed electric-current pressure intering (PECPS) of sol-gel derived solid solution powders", *Processing and Properties of Advanced Ceramics and Composites VI,* **249**, (The American Ceramic Society,Ohio, 2014) pp. 3-13.

11) T. Tsukigata and K. Tsukuma, "Zirconia powder - raw material for the fabrication of high strength and high toughness zirconia ceramics", Ceramics, **17,** 816-822 (1982).

12) K. Yamamoto, M. Kato, K. Hirota, H. Taguchi, H. Kimura, T. Kunisada, Y. Kageyama, and H. Morita: "Fabrication of High Strength and Toughness Ceramics Using Pulsed Electric-Current Pressure Sintering of $ZrO_2(Y_2O_3)$-Al_2O_3 Solid Solution Powders Prepared by the Neutralization of Co-Precipitation Method", J. Jpn. Soc. Powder Powder Metall., **60**, 428-435 (2013).

13) T. Tsukuma, K. Ueda, and M. Shimada, "Strength and fracture toughness of isostatically hot-pressed composites of Al_2O_3 and Y_2O_3-partially-stabilised ZrO_2", J. Am. Ceram. Soc., **68,** C-4 ~ C-5 (1985).

14) S. Hori, M. Yoshimura and S. Somiya, "Strength-toughness relations in sintered and isostatically hot-pressed ZrO_2-toughned Al_2O_3", J. Am. Ceram. Soc., **69**, 169-172 (1986).

15) K. Tsukuma, K. Ueda, K. Matsushita, and M. Shimada, "High-temperature strength of Y_2O_3-partially-sabilized ZrO_2/Al_2O_3 composites", J. Am. Ceram. Soc., **68**, C-56 ~ C-58 (1985).

16) R. Shikata, Y. Urata, T. Shiono, and T. Nishikawa, "Strengthening of Y-PSZ-Al_2O_3 composite ceramics", J. Jpn. Soc. Powder Powder Metall., **37,** 357-361 (1990).

17) R. C. Garvie and P. S. Nicholson, "Phase analysis in Zirconia Systems," J. Am. Ceram. Soc., **55,** 303-305 (1972).

18) M. I. Mendelson, "Average Grain Size in Polycrystalline Ceramics", J. Am. Ceram.Soc., **52,** 443-446 (1969).

19) I. Nakai and F. Izumi, *Powder X-ray diffraction analyisis-2nd ed.*, (Asakura-Shoten, Tokyo, 2009).

20) K. Niihara, R. Morena, and D. P. H. Hasselman, "Evaluation of K_{IC} of Brittle Solids by the Indentation Method with Low Crack-to-Indent Ratios", J. Mater. Sci. Lett., **1** ,13-16 (1982).

21) K. Hirota, H. Sato, K. Takaoka, M. Kato, and H. Taguchi, "Fabrication of high strength and high toughness $ZrO_2/25mol\%Al_2O_3$ composite ceramics using high-pressure (1 GPa) sintering", The Soc. Mater. Sci. Jpn., **61,** 419-425 (2012).